JOURNAL OF GUIDANCE, CONTROL, AND DYNAMICS
Vol. 15, No. 3, May-June 1992

Local Control Design Methodologies for a Hierarchic Control Architecture

Jonathan P. How and Steven R. Hall
Massachusetts Institute of Technology, Cambridge, Massachusetts 02139

Active structures such as smart skins or optical mirrors require high densities of sensors and actuators to achieve the performance objectives. The problems associated with the design and implementation of controllers for this type of active structure have previously led to the development of a hierarchic control architecture. The approach combines a centralized global controller based on aggregate structural information and a distributed set of residual, or local, controllers in a two-level architecture that removes many of the design and implementation difficulties. Three decentralized methodologies that are suitable for implementation as local controllers in the hierarchic architecture are developed and analyzed in this paper. The approaches are distinguished by the communication constraints imposed during the control design. Consistent with many applications for smart skins and typical mirror designs, these controllers are developed for structures that exhibit a high degree of spatial symmetry. The simplest design employs collocated feedback. A second technique constrains the exchange of information to be within isolated regions of the structure. The third approach permits communication between adjacent local controllers. Simulation results from the control of a long beam in bending are used to compare these local control design methodologies in terms of both the overall performance and implementation requirements.

Nomenclature

A,B,C,D = state-space system matrices
A_i = blocks of a circulant matrix
e = residual interpolation error
$F_{(\cdot)}, f_{(\cdot)}(z)$ = feedback gain matrices
h_g = number of nodes per finite control element, $= n/n_e$
K,M = finite element model stiffness and mass matrices
m_l = mass within local region of structure
N = number of subsystems in a circulant model
n = number of degrees of freedom in condensed finite element model
n_e = number of finite control elements
n_g = number of global degrees of freedom
$n_{g_{\text{dof}}}$ = number of degrees of freedom per global node
n_l = number of global modes retained
P,Q = Lyapunov equation solution matrices
Q_g, Q_e = generalized forces
q = finite element model degrees of freedom
R_{xx}, R_{uu} = linear quadratic regulator state, control weights
S_g, S_e = force distribution matrices
T_g, T_r, T_{gl} = interpolation matrices
u = control inputs
u_e = residual control inputs
u_r = u_e after spatial filtering
Φ_n = circulant transformation matrix based on I_n, an $n \times n$ identity matrix
ϕ_g = mode shapes of the global model in the global coordinate system
Ψ = control influence matrix
ω_N^m = $e^{2\pi jm/N}$

Jonathan P. How received his B.A.Sc. in Engineering Science (Aerospace Option) from the University of Toronto in 1987 and his S.M. in Aeronautics and Astronautics from the Massachusetts Institute of Technology in 1990. He is currently working on his Ph.D. at M.I.T. Current research interests include control architecture designs for large-scale flexible structures, with special applications to deformable mirror control for adaptive optics. He is a Student Member of AIAA.

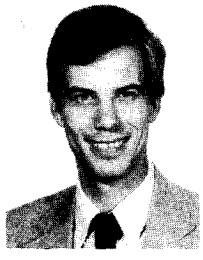

Steven R. Hall received his S.B., S.M., and Sc.D. degrees from the Massachusetts Institute of Technology, Department of Aeronautics and Astronautics, in 1980, 1982, and 1985, respectively. Since 1985, he has been on the faculty at M.I.T., where he is currently the Finmeccanica Career Development Associate Professor of Aeronautics and Astronautics. His research interests include active control of flexible structures and the control of helicopter vibration and rotor dynamics. He is a Senior Member of AIAA.

Received July 2, 1990; revision received Feb. 20, 1991; presented as Paper 91-2806 at the AIAA Guidance, Navigation, and Control Conference, New Orleans, LA, Aug. 12-14, 1991; accepted for publication Sept. 25, 1991.

Subscripts

$g;r,e$ = global and residual model, respectively
$gg,.,rr$ = transformed system matrices for M and K

Superscripts

$-$ = circulant transformed representation
H = Hermitian

Introduction

THE objective of eliminating the unwanted vibratory motion of a structure is recognized as being a particularly difficult one, in part because of the physical characteristics of the plant, which are typically large and lightly damped.[1] These difficulties are compounded by an increase in the performance requirements associated with the missions envisioned for many future spacecraft. For space-based telescopes and interferometers, stringent performance requirements require high control bandwidths, so that flexible modes have a significant influence on the objectives.[2-4] It is of interest to note that these phenomena are also a factor in large Earth-based telescopes.[5]

Structures for optical systems are especially challenging because meeting the performance objectives to the degree of spatial resolution typically required demands a large number of sensors and actuators.[6-10] An important issue for these structures is how to design the control architecture to handle the large amount of information that is available. These so-called intelligent structures, with many densely packed actuators and sensors, have been made possible by the use of piezoelectric ceramic and piezopolymer film materials as the sensing and actuating devices.[7,11-14] The feasibility of reliable real-time parallel-processing computer architectures has been significantly enhanced by the advances made in the field of robotic vision.[15]

A control architecture designed to handle the difficulties associated with the control of a space structure with a large number of sensors and actuators is presented by Hall et al.[16] The architecture achieves a computationally feasible design by splitting the regulation effort between two levels of controllers. Reference 16 compares the approach to a variety of centralized and distributed designs. It is demonstrated that the multilevel architecture incorporates into one design most of the benefits (i.e., parallel in nature), but not all of the disadvantages (i.e., retention of a large global control authority) of both the centralized and decentralized schemes. The resulting hierarchic control architecture compares favorably to the multilevel designs obtained via the interaction prediction or goal coordination methods[17] because of the significant reduction in the amount of information transmitted between the different control levels. Designs based on these two approaches typically require that all state measurements from each subsystem be transmitted to a central coordinator. The approach of Ref. 16 only requires that aggregate values of these measurements be communicated. As will also be seen, in the use of structural coherency arguments to split the system and aggregate variables to design the controllers, the hierarchic controller discussed here is related to Chow's work in Ref. 18 for power networks.

Hall et al.[16] analyze the control architecture only for the simplest lower-level control design. The aim of this paper is to extend the analysis to determine the advantages and disadvantages of incorporating more sophisticated (measured by the amount of information back) local controllers at the lower level of the architecture. Three approaches that are distinguished by the constraints imposed on the allowable exchange of information are compared. It is to be expected that the more information available to a controller, the better the achievable performance and the higher the implementation costs. The goal here is to quantify this statement and, thus, determine the tradeoffs between achievable performance and implementation costs as more sophisticated local controllers are employed. Implementation costs include both the number of computations required and the amount of information transferred between the processors associated with regions of the structure called finite control elements (FCE).

The following section briefly discusses the hierarchic control architecture, giving an overview of the approach originally presented in Ref. 16. The next section provides three local control designs from How.[19] For simplicity in the comparison, the computational requirements are evaluated for state feedback using three types of constraints on the local control design. The resulting controllers are then applied to a simple model, and the performance and number of computations required for each technique are compared. As will be discussed in the next two sections, for actual implementation, the techniques used here could be developed for dynamic compensators enforcing, for example, a high-frequency rolloff.

Hierarchic Control Architecture

The control architecture was originally developed by Ward[20] and expanded by Hall et al.[16] and How.[19] The fundamental idea behind the control formulation is to develop a parallelism between the element/global hierarchy of the structural model and the regional/global hierarchy of the active control.

The motion of a finite-dimensional evaluation model of the structure can be represented by the degrees of freedom q_{eval}. The full finite element model (FEM) is then condensed to one in which the structure is represented by an aggregate of these degrees of freedom, namely q, each of which is associated with an actuator (and collocated sensor).[21] In the case of an intelligent structure, with numerous sensors and actuators, this condensation will still yield a fairly accurate structural model. The structure is subdivided into an appropriate number of FCEs that are associated with several of the degrees of freedom q. The coordinates of a coarser model of the structure are located at the boundaries of the FCEs and represent the degrees of freedom of the global model q_g. The vectors q and q_g are related in Eq. (2) by an interpolation matrix T_g.

Figure 1 illustrates the division of control effort in the hierarchic architecture. The three basic tasks to implement the global control are 1) the aggregation to reduce q to states of the global model q_g, 2) the computation of the global control commands Q_g, and 3) the distribution of the global control. In terms of the implementation, it is beneficial to perform the aggregation and distribution tasks cooperatively at both the global and local levels.

The regional controllers are most efficiently implemented when each is associated with an FCE. The local controllers act on the residual e, the error between the actual measurements q, and an interpolation of the local estimates from the global states q_g. The specific objective of the regional controllers is to perform inner-loop compensation in order to force the structure to track the behavior expected by the global model. The filtering of u_e to obtain u_r ensures that the global modes are not excited by the residual control. The total control u applied

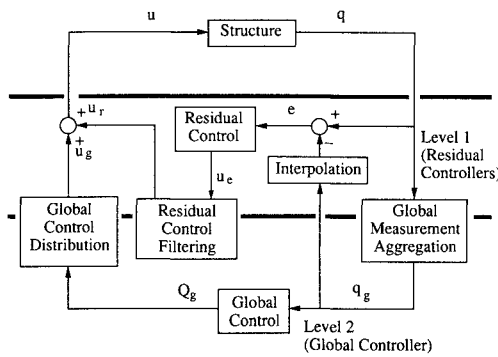

Fig. 1 Division of control functions in a two-level hierarchic controller. The measurement aggregation, control distribution, and residual filtering tasks are shared between the two levels.

to the structure is then an addition of the distributed global control u_g and the filtered local control u_r.

The condensed dynamics of an undamped structural model can be written as

$$M\ddot{q} + Kq = \Psi u = \Psi(u_g + u_r) \tag{1}$$

To define the global and residual degrees of freedom, the displacements of the condensed model are written as a sum of the interpolated displacements of the global model and a vector of n residuals

$$q = T_g q_g + e \tag{2}$$

where $q_g \in R^{n_g}$, $T_g \in R^{n \times n_g}$, and $e \in R^n$, and similarly for the velocity degrees of freedom. Minimizing a quadratic function in e, weighted by the mass M, establishes that the global degrees of freedom are related to the condensed degrees of freedom by

$$q_g = (T_g^T M T_g)^{-1} T_g^T M q = T_g^{-L} q \tag{3}$$

where superscript $-L$ denotes the left pseudoinverse. The $n_r = n - n_g$ independent degrees of freedom of e, designated q_r, may be expressed as

$$e = T_r q_r \tag{4}$$

where the matrix $T_r \in R^{n \times n_r}$ is yet to be determined. Equation (2) can then be rewritten as

$$q = T_g q_g + T_r q_r = \begin{bmatrix} T_g & T_r \end{bmatrix} \begin{bmatrix} q_g \\ q_r \end{bmatrix} \tag{5}$$

Note that the columns of T_r are not unique and may be determined by performing a Gram-Schmidt orthogonalization on any set of n_r columns that, when combined with the columns of T_g, form a linearly independent set.

The complete control is a combination of the two inputs u_g and u_r, which are physical forces based on the commands Q_g and Q_e. These pairs are related through force distribution matrices

$$u_g = S_g Q_g, \qquad u_r = S_e Q_e \tag{6}$$

In the case of Ψ invertible, appropriate selections for these distribution matrices to decouple the control influence of the subsystems are

$$S_g = \Psi^{-1} M T_g (T_g^T M T_g)^{-1} = \Psi^{-1} T_g^{-LT} \tag{7}$$

$$S_e = \Psi^{-1} M T_r (T_r^T M T_r)^{-1} T_r^T = \Psi^{-1} T_r^{-LT} T_r^T \tag{8}$$

Employing state feedback at both levels, the form of the feedback laws is

$$Q_g = -F_g q_g - F_{\dot{g}} \dot{q}_g, \qquad Q_e = -F_e e - F_{\dot{e}} \dot{e} \tag{9}$$

These relationships can be substituted into Eq. (1) and premultiplied by $[T_g \;\; T_r]^T$ to give

$$\begin{bmatrix} M_{gg} & 0 \\ 0 & M_{rr} \end{bmatrix} \begin{bmatrix} \ddot{q}_g \\ \ddot{q}_r \end{bmatrix} + \begin{bmatrix} K_{gg} & K_{gr} \\ K_{rg} & K_{rr} \end{bmatrix} \begin{bmatrix} q_g \\ q_r \end{bmatrix}$$

$$= -\begin{bmatrix} F_g & 0 \\ 0 & T_r^T F_e T_r \end{bmatrix} \begin{bmatrix} q_g \\ q_r \end{bmatrix} - \begin{bmatrix} F_{\dot{g}} & 0 \\ 0 & T_r^T F_{\dot{e}} T_r \end{bmatrix} \begin{bmatrix} \dot{q}_g \\ \dot{q}_r \end{bmatrix} \tag{10}$$

where the mass and control influence matrices are completely uncoupled, and the stiffness matrix is uncoupled to the extent that T_g models n_g of the modes of the condensed finite dimensional system.[16]

The effect of the global and residual control on the condensed model can also be determined by substituting Eqs. (3) and (6–9) into Eq. (1) and using the identity

$$T_r T_r^{-L} = I - T_g T_g^{-L} \tag{11}$$

to obtain

$$M\ddot{q} + Kq = -\left\{T_g^{-LT} F_g T_g^{-L} + (I - T_g T_g^{-L})^T F_e (I - T_g T_g^{-L})\right\} q$$

$$- \left\{T_g^{-LT} F_{\dot{g}} T_g^{-L} + (I - T_g T_g^{-L})^T F_{\dot{e}} (I - T_g T_g^{-L})\right\} \dot{q} \tag{12}$$

This representation suggests the control architecture shown in Fig. 2. Path "o" is the process that filters the global motion from the overall motion to form the residual (observation filtering). Path "c" is the process that filters the global component out of the residual commands (control filtering). Note that, because of Eq. (11), it is not necessary to explicitly calculate T_r or to determine q_r. Equation (12) demonstrates that the hierarchic control architecture is equivalent to a full gain matrix with a prespecified internal structure. Converting to a frequency domain representation, it is clear that one can incorporate a dynamic compensator at the lower level by replacing the constant matrices F_e and $sF_{\dot{e}}$ with $F_e(s)$ and $sF_{\dot{e}}(s)$ in Eq. (12).

One technique to minimize the K_{gr} stiffness coupling term in Eq. (10) is to retain only the n_l lower-frequency modes of the global model, written as ϕ_g^l. All of these results then hold with this selection if the modified interpolation function $T_{gl} \equiv T_g \phi_g^l$ is substituted for T_g.

Local Control Design Methodologies

The hierarchic architecture separates the effort between two controllers that are distinguished by the level of control authority that they exert on the structure. The centralized global controller is designed for performance on low-frequency modes of the structure, and the distributed local controllers of the lower level are designed to complement this performance for the structure under consideration. In particular, these local controllers regulate the short wavelength vibrations that are rendered unobservable to the central controller by the spatial filtering of the architecture in Fig. 2. In damped structures, the higher-frequency motions tend to have short correlation length scales, resulting in strongly banded static feedback gains, which is consistent with the goal of a localized lower-level controller for the architecture.

The performance objective for the local control designs is obtained from the global objective by retaining only those terms to which the short wavelength motions have a significant contribution. Skelton et al.'s[22] modal cost analysis (MCA) provides a convenient measure of the contribution of structural modes to the performance objective. The particular example discussed in this paper considers the shape control of

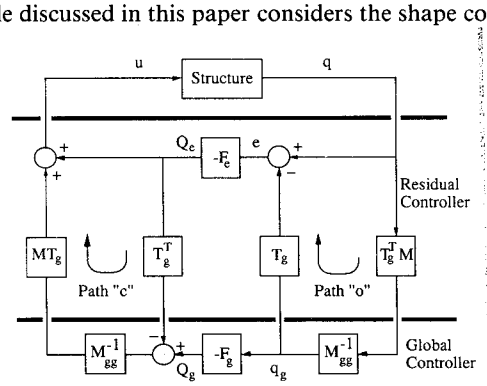

Fig. 2 Representation of the hierarchic control architecture showing the division of control effort between the two levels. Path "o" is the observation filtering step and path "c" is the control filtering.

a mirror-like surface, an appropriate global performance objective combines line-of-sight (LOS) endpoint displacement errors, an overall measure of the displacement error at each node, and the total energy of the structure. Performing MCA for a combination of these objectives on a Bernoulli-Euler beam model indicates that only the latter two terms are significant for higher-frequency vibrations.

A discussion of the implementation of a local control design must include an analysis of the communication and computational requirements for the approach. For state feedback controllers, the bandwidth of the gain matrix is an appropriate measure of both the number of calculations required and the distance over which the sensor measurements must be communicated. Reducing the bandwidth of the gain matrix for a controller decreases both the communication and computational requirements for that design. However, the question of the influence of the bandwidth on the achievable performance still remains.

Three approaches to the design of static local controllers are analyzed to study this question. These methodologies employ diagonal, block diagonal, and block tridiagonal feedback gain matrices, as shown schematically in Fig. 3. Diagonal feedback corresponds to the case that minimizes the exchange of information. The block diagonal and block tridiagonal cases are more sophisticated in that they allow information to be exchanged, but they differ by the range over which the exchange can occur. The block diagonal form limits feedback to within an FCE, whereas the block tridiagonal form limits communication to between neighboring FCEs. A fourth design with a full gain matrix based on a highly distributed implementation of the optimal centralized controller is considered in Ref. 19. However, the results for this last design depend almost exclusively on the communication rate between processors, which is a direct function of the computer architecture and, thus, too specific for the present analysis.

The subsequent sections outline the three design approaches for structures with a high degree of spatial symmetry, a choice that was motivated by mirror, antennas, and many other smart skins applications.[1,7,10] The requirement of high spatial resolution for optical quality mirrors results in a high density of sensors and actuators, and so the assumptions regarding intelligent structures hold for these devices. The objective of the study is to accumulate, for the purposes of comparison, the communication, computation, and performance results for several designs with various feedback gain matrix bandwidths. For simplicity, a symmetric beam is used in the designs. For other assumptions about the symmetry of the structure, different design approaches would have to be developed. As mentioned, for simplicity in the comparison, only state feedback controllers have been considered.

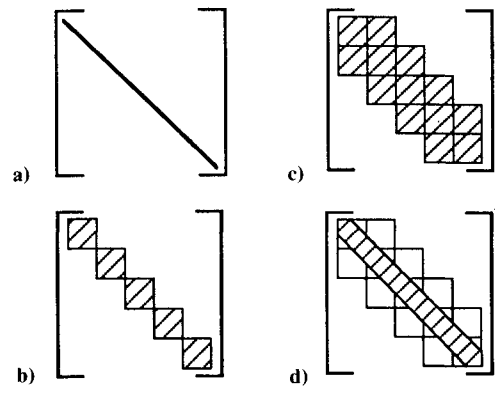

Fig. 3 Schematic comparison of the matrix bandwidth for static feedback gains: a) diagonal gain of collocated feedback; b) block diagonal; c) full block tridiagonal feedback; d) banded block tridiagonal case.

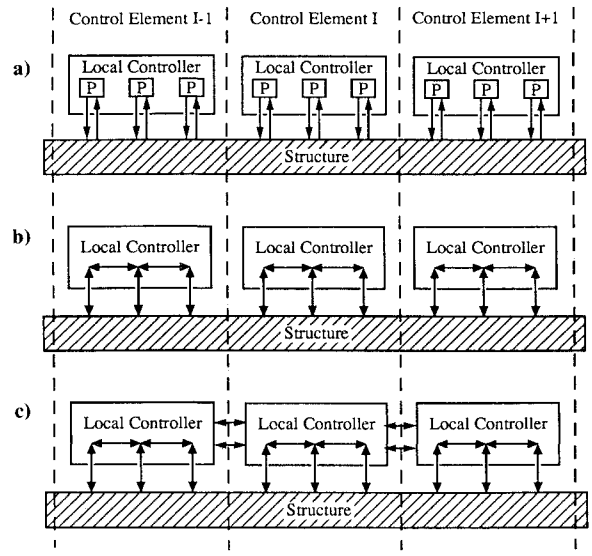

Fig. 4 Representation of local control designs: a) collocated; b) block diagonal, sensor information is exchanged within isolated regions; c) block tridiagonal, information is exchanged between neighboring controllers.

Collocated Feedback

Collocated feedback is the simplest of the four designs because the feedback gains are purely diagonal. The generic form of the control with state and rate feedback is

$$u(z) = -f_q(z)q - f_{\dot{q}}(z)\dot{q} \tag{13}$$

using z to indicate the spatial coordinate. A particular form of Eq. (13) suggested by Silverberg[23] is

$$u = -\beta^2 m_l q - 2\beta m_l \dot{q} \tag{14}$$

where m_l is a measure of the local mass of the structure, and the gains are equal for each position z. Feedback of the form in Eq. (14) is categorized as a natural control design since the open-loop mode shapes are unchanged by the implementation of the control. Equation (14) also results in uniform damping since each closed-loop pole is moved to the vertical line $\mathrm{Re}(s) = -\beta$ in the complex plane. The parameter β is typically selected to provide a sufficient level of damping to robustly stabilize higher-frequency modes of the model.[24]

A schematic of the local controller is shown in Fig. 4a. There are several independent feedback loops associated with each FCE. The feedback within each FCE can be implemented as several single-input single-output (SISO) analog circuits, or as a single digital processor with multiple SISO channels. In the notation of the figures, each box denotes a complete controller and each processor (P) is associated with a single SISO loop.

Several studies of collocated feedback have demonstrated its robustness to modeling errors and that it can be used to supplement the damping of high-frequency, poorly modeled modes.[25,26]

Circulant Design of Decentralized Controllers

The next level of sophistication in the local control designs is to allow each control command in an FCE to be calculated using all of the information measured within that region of the structure. Two main approaches exist in the literature for solving this decentralized control problem.[27] In the first method, the structure is decomposed into isolated subsystems, and independent control designs are performed on each. These decomposition approaches ignore the connections between the subsystems, and can, except for the very weakly coupled cases, result in relatively poor performance, if not instability.[28] In contrast, the second approach employs a design model that

includes the coupling, but with constraints on the allowable exchange of information between controllers. The second approach is used here since it is known that the subsections of a beam model are strongly coupled.

Two sizes of block diagonal controllers are analyzed. One is designed for the full FCE. The other is designed for a bay one-half the size of the FCE and is referred to as the two-bay block diagonal design. Since this second design explicitly incorporates communication restrictions within an FCE into the approach, it provides a further data point and, thus, improves the comparison of the cost and performance tradeoffs. Figure 4b illustrates the form of the block diagonal decentralized controller.

In these designs, the aim is to develop a controller that can only feedback the states from within a region of the structure. Using N FCEs, the static feedback equation is

$$\begin{bmatrix} u_1 \\ u_2 \\ \vdots \\ u_N \end{bmatrix} = - \begin{bmatrix} F_{q1} & 0 & \cdots & 0 \\ 0 & F_{q2} & & 0 \\ \vdots & & \ddots & \\ 0 & 0 & & F_{qN} \end{bmatrix} \begin{bmatrix} q_1 \\ q_2 \\ \vdots \\ q_N \end{bmatrix}$$

$$- \begin{bmatrix} F_{\dot{q}1} & 0 & \cdots & 0 \\ 0 & F_{\dot{q}2} & & 0 \\ \vdots & & \ddots & \\ 0 & 0 & & F_{\dot{q}N} \end{bmatrix} \begin{bmatrix} \dot{q}_1 \\ \dot{q}_2 \\ \vdots \\ \dot{q}_N \end{bmatrix} \tag{15}$$

where q_i and u_i represent the vectors of the states and control for each element, and the F_{q_i} are appropriately sized block matrices. The problem is to calculate F_{q_i} and $F_{\dot{q}_i}$ in Eq. (15) to optimize a performance objective based on the global cost just discussed.

The optimization problem for the constrained architecture feedback is very similar to the output feedback problem developed by Levine and Athans[29] in that the extra constraint on the form of the feedback matrices couples the necessary conditions. Many papers have addressed the issue of a numerical solution of coupled matrix equations,[29-32] but solving these equations for a large-scale system is very difficult. The technique discussed here uses the symmetry of the structure to reduce the plant dimension (and consequently the order of the matrix equations) to a more manageable level. The approach is based on a discrete spatial Fourier transform (DFT) of the structural model. Chu[33] employed the technique on a system described by an infinite string of identical subsystems. Brockett and Willems[34] demonstrated the benefits of the approach for systems with circulant symmetry. Wall[35] extended the analysis to include the control and estimation of large-scale, spatially symmetric systems using both circulant and toeplitz models. More recently, the technique has been employed in the continuous sense by applying a Fourier decomposition directly to the differential equations of a structural model.[36] Lunze[37] employs a similar technique for a power system modeled as a collection of symmetrically coupled subsystems.

The solution procedure employed here consists of several steps. The first is to model the structure as a circulant system. A block circulant matrix of order N can be written as[35]

$$A = \begin{bmatrix} A_0 & A_{N-1} & A_{N-2} & \cdots & A_1 \\ A_1 & A_0 & A_{N-1} & & A_2 \\ A_2 & A_1 & A_0 & & A_3 \\ \vdots & & & \ddots & \\ A_{N-1} & A_{N-2} & A_{N-3} & & A_0 \end{bmatrix} \tag{16}$$

where $A_i \in R^{n_1 \times n_2}$, so the blocks of A need not be square. The dynamics of an Nth-order block circulant system with r states, s control inputs, and t sensors per subsystem are

$$\begin{aligned} \dot{x} &= Ax + Bu \\ y &= Cx + Du \end{aligned} \tag{17}$$

where $A \in R^{Nr \times Nr}$, $B \in R^{Nr \times Ns}$, $C \in R^{Nt \times Nr}$, and $D \in R^{Nt \times Ns}$ are block circulant matrices. Note that the number of subsystems N is typically much larger than the dimensions of each subsystem r. The important properties of a circulant system are that each subsystem has the same internal dynamics A_0 and that the influence of any one subsystem on another is only a function of their relative separation.

Simple examples of circulant systems are circular plates with pie-shaped subsystems, or a ring of hexagonal plates. In both cases, the system is in the form of a circularly symmetric ring of subsystems that are connected to meet the restrictions just given. To approximate a beam as a circulant system, it is necessary to assume that the two ends are connected, a valid approximation if the beam is long in comparison to the region of influence of the boundary conditions. It is necessary to check both the validity of this assumption a posteriori in the model, and the performance of the resulting control design in the neighborhood of the beam endpoints. For more general structures, an embedding procedure described by Brockett and Willems[34] would lead to a more accurate model, but the technique nearly doubles the system dimension.

At this point, the model consists of N coupled $r \times r$ subsystems, with the overall dynamics governed by system matrices of the form given in Eq. (16). In the following development, each subsystem is associated with an FCE. The purpose of the next step in the synthesis is to employ a block similarity transform to obtain a block diagonal representation of the coupled system in Eq. (17). The transformation can be physically motivated as a spatially discrete Fourier transform based on the transformation matrix

$$\Phi_k = I_k \otimes \begin{bmatrix} 1 & 1 & \cdots & 1 \\ 1 & \omega_N & & \omega_N^{N-1} \\ \vdots & & \ddots & \\ 1 & \omega_N^{N-1} & & \omega_N^{(N-1)(N-1)} \end{bmatrix} \tag{18}$$

where the exponent of ω_N is a measure of the relative spatial separation of the subsystems, and $\otimes$ is the Kronecker product.[38] As discussed in Wall,[35] applying the transformation to the states, controls, and sensors of the model

$$\bar{x} = \Phi_r^{-1} x, \qquad \bar{u} = \Phi_s^{-1} u, \qquad \bar{y} = \Phi_t^{-1} y \tag{19}$$

yields a new representation of the circulant system of Eq. (17)

$$\begin{aligned} \dot{\bar{x}} &= \bar{A}\bar{x} + \bar{B}\bar{u} \\ \bar{y} &= \bar{C}\bar{x} \end{aligned} \tag{20}$$

where each of the transformed matrices denoted as $(\bar{\cdot})$ is block diagonal, and for simplicity in the following, the system matrix D is taken to be zero. Employing the DFT reduces the circulant model to N decoupled $r \times r$ subsystems in a spatial frequency domain representation.

The third step in the analysis is to formulate and reduce the order of the control synthesis problem. It is assumed that the state and control weighting matrices can be expressed in block circulant form, as is the case for the displacement, velocity, and energy weights typically used for low authority control. The decoupling of the control problem relies on the observation that the DFT can also be applied directly to Lyapunov and

Riccati equations to obtain a block diagonal form.[35] To formulate the necessary conditions, the transformed cost function is augmented with the constraints and then differentiated with respect to elements of the matrices $\bar{P}$, $\bar{Q}$, and the free blocks of the gain matrix F (set of indices denoted by α). The resulting equations are

$$(\bar{A}_i - \bar{B}_i\bar{F}_i\bar{C}_i)\bar{Q}_i + \bar{Q}_i(\bar{A}_i - \bar{B}_i\bar{F}_i\bar{C}_i)^H + \bar{\Sigma}_i = 0 \tag{21}$$

$$\bar{P}_i(\bar{A}_i - \bar{B}_i\bar{F}_i\bar{C}_i) + (\bar{A}_i - \bar{B}_i\bar{F}_i\bar{C}_i)^H\bar{P}_i + \bar{R}_{xx_i} + \bar{C}_i^H\bar{F}_i^H\bar{R}_{uu_i}\bar{F}_i\bar{C}_i = 0 \tag{22}$$

$$\sum_{i=0}^{N-1} (\bar{C}_i\bar{Q}_i\bar{C}_i^H\bar{F}_i^H\bar{R}_{uu_i} - \bar{C}_i\bar{Q}_i\bar{P}_i\bar{B}_i)\omega_N^{-ik} = 0, \quad \forall k \in \alpha \tag{23}$$

where $\overline{A^T} = \bar{A}^H$, $\overline{R^{-1}} = \bar{R}^{-1}$, and $(\bar{\cdot})_i$ is the ith diagonal block of $(\bar{\cdot})$; $\bar{\Sigma}$ is the covariance of the initial states. The necessary conditions are coupled in this frequency domain representation because of the a priori specification of the gain structure. Referring to the form of a circulant matrix in Eq. (16), if every block of the gain matrix F is free, $\alpha = \{0,1,\ldots,N-1\}$, and Eqs. (21-23) reduce to the normal set of three coupled matrix equations for the output feedback problem.[29] For the special case of a block diagonal gain matrix, $\alpha = \{0\}$, $\bar{F}_k = F_0 \forall k$, and the summation in Eq. (23) is simplified since $\omega_N^{-ik} = 1 \forall i$.

The spatial transformation reduces the (Nr)th-order problem to N, rth-order problems. Since the solution of a Lyapunov equation is at least an r^3 operation, it is clear that the transformation considerably reduces the number of computations required. This is a particularly important point considering the role of the Lyapunov equation in the numerical solution procedure.[19,39] The overhead in forming the transformed system representation can be implemented efficiently as a fast Fourier transform (FFT), which is an $r^2 \log_2 r$ operation[40] and is performed only once.

The DFT approach can also be applied to determine circulant dynamic compensators. The dynamic equivalent of Eqs. (21-23) would then provide a computationally efficient means of designing a series of identical compensators that yield superior performance in the presence of sensor and actuator noise or model uncertainty. An interesting extension of this synthesis technique would be to develop symmetric, robust decentralized controllers such as those designed for the nonsymmetric case in Ref. 41.

In the block diagonal case, one controller F_0 is designed to stabilize each of the N subsystem models $(\bar{A}_i, \bar{B}_i, \bar{C}_i, \bar{R}_{xx_i}, \bar{R}_{uu_i})$. The synthesis procedure is closely related to the multiple-objective, multiple-model control design procedure discussed in Ref. 42 for the case where each plant model is equally likely to occur and the system matrices are complex. Employing the same control algorithm at each processor is significantly simpler to implement, but examples with dynamic compensators have indicated that this extra assumption can result in a suboptimal overall design.

Gradient and Newton numerical search algorithms were employed to find the minimizing solution of Eqs. (21-23). A quasi-Newton method was also investigated, but examples indicated rather poor convergence properties. The results of several optimization examples are available in Ref. 19, but they are not central to the following discussion.

Distributed Control with Communication

The next level of sophistication in the local control designs is to share sensor information between processors. In the limit, as the number of controllers from which information can be received increases, it is possible to obtain a decentralized implementation of a centralized controller. However, in these designs, the exchange of information is restricted to occur only between the processors of adjacent elements, hence the name block tridiagonal feedback.

Two main approaches are available to exchange the sensor measurements. One approach is to measure locally and communicate the information to neighbors (Fig. 4c). The second is to directly measure the sensors from its own and neighboring FCEs.

Each approach has advantages, and a more complete comparison would illustrate the tradeoff between having the extra measurement hardware built into the structure and having to perform local communication between processors.[43] The second technique is more difficult to implement, as several processors need to measure each sensor, but little local coordination between the controllers is required. The first approach is more compact, but it has the major disadvantage that it requires the local controllers to be coordinated and, thus, dedicate some portion of their operation cycle to sending and receiving information from neighboring processors. There are delay issues involved here as well, as some information is transferred rather than directly measured.

An important subset of the block tridiagonal gain matrices is the case of a banded gain matrix, where the bandwidth is selected to be small enough that only one extra set of off-diagonal block matrices is required (Fig. 3d). If the bandwidth is smaller than the FCE size, then, as is shown in the figure, only a small fraction of the three block matrices in a given row need be nonzero. This technique reduces the amount of information passed from processor to processor, or alternatively, how far into adjacent elements extra measurements must be obtained.

The static feedback equation now is

$$\begin{bmatrix} u_1 \\ u_2 \\ u_3 \\ \vdots \\ u_N \end{bmatrix} = - \begin{bmatrix} F_{1_{q_1}} & F_{1_{q_2}} & 0 & \cdots & 0 \\ F_{2_{q_1}} & F_{2_{q_2}} & F_{2_{q_3}} & & 0 \\ 0 & F_{3_{q_2}} & F_{3_{q_3}} & & 0 \\ \vdots & & & \ddots & \\ 0 & 0 & 0 & F_{Nq_{N-1}} & F_{Nq_N} \end{bmatrix} \begin{bmatrix} q_1 \\ q_2 \\ q_3 \\ \vdots \\ q_N \end{bmatrix} - \begin{bmatrix} F_{1_{\dot{q}_1}} & F_{1_{\dot{q}_2}} & 0 & \cdots & 0 \\ F_{2_{\dot{q}_1}} & F_{2_{\dot{q}_2}} & F_{2_{\dot{q}_3}} & & 0 \\ 0 & F_{3_{\dot{q}_2}} & F_{3_{\dot{q}_3}} & & 0 \\ \vdots & & & \ddots & \\ 0 & 0 & 0 & F_{N\dot{q}_{N-1}} & F_{N\dot{q}_N} \end{bmatrix} \begin{bmatrix} \dot{q}_1 \\ \dot{q}_2 \\ \dot{q}_3 \\ \vdots \\ \dot{q}_N \end{bmatrix} \tag{24}$$

where q_i and u_i are defined as before, and F_{kq_i} is the gain matrix for processor k from the state component q_i. For the tridiagonal restriction, $i \in \{k-1, k, k+1\}$ since only the diagonal and closest neighbor gain blocks are nonzero. No restriction is made on the actual structure within the gain blocks, just on the blocks that are nonzero, and so the purely banded case is also included.

As with the preceding design, there exist several techniques to solve for the block gain matrices. One approach is to use the previously derived DFT circulant model method, with the nonzero gain blocks in Eq. (23) given by the set $\alpha = \{N-1, 0, 1\}$. The resulting summation is more complicated, but the solution procedure is exactly the same as the block diagonal case. A second, somewhat simpler approach exists if it is known that the gain matrices are strongly banded. In this case, it is possible to truncate the gains with a small, known error to obtain the desired structure given earlier. The gains obtained for the examples investigated here, which use energy or displacement weightings for a beam, possess a high degree of bandedness, and so this second aproach is a viable alternative. However, since the full feedback gains are computationally intensive to calculate for large-scale systems, an alternative technique for calculating the gains for structures that possess a high degree of spatial symmetry is required. The

technique discussed here is an extension of the DFT approach already discussed.

The first step in the approach is to select a repeated bay of the structure that includes a single sensor and actuator pair. As with the circulant case, a DFT is employed to express the model in terms of a reduced model whose dimension is governed by the size of the repeated bay. These reduced-order models are also parameterized by a complex index variable. As in the approach to the block diagonal design, the DFT is also applied to the control problem, and the optimal gains for the SISO problem are obtained as a function of the index variable. Inverse transforming the gains expresses them as a function of the spatial coordinate, and by symmetry, these gains can be used at each internal actuator location to form the full gain matrices. The gain matrices can then be truncated to meet either the banded or full block tridiagonal restrictions. The final step is to check the assumptions of the bandedness of the control matrix gains and to calculate the gains for the control locations strongly influenced by the boundary conditions.

Computational Requirements

The final part of the comparison is a discussion of the computational requirements for the local controllers. The results are presented for the special case of a static feedback hierarchic control architecture applied to a one-dimensional structure. In general, it is not assumed that the nodes of the global model coincide with structural nodes, but it is assumed that the internal FCEs are identical, with h_g nodes between the global nodes. The FCEs at either end then have $h_g - 1$ internal nodes and one structural node that coincides with a global node (Fig. 5).

The total computational requirements consist of the overhead associated with the architecture and the implementation of the feedback algorithm. For each global iteration, the central controller, assuming static feedback of $\boldsymbol{q}_g$ and $\dot{\boldsymbol{q}}_g$, must perform approximately $5n_g^2$ multiplications and additions (approximately one-third of a multiplication). The architecture overhead for each local controller is $12n_{g_{\text{dof}}}h_g$ multiplications and additions. Since the architectural computations are performed at the slower, central controller update rate, the contributions for these two parts are listed separately. Examples of the requirements for various local control static feedback laws are given in Table 1.

Discussion of Results

The next step in the comparison is to apply the hierarchic control design procedure to an example of a beam in bending. For simplicity, the analyzed structure is a 30-node beam (Fig. 5). The evaulation FEM includes both the displacement and rotational degrees of freedom at each node. Consistent with the assumptions of an intelligent structure, displacement sensors (differentiated to get velocity) with a collocated force actuator are used at each node for this simple example. Only the displacement degrees of freedom are retained in the design model ($n = 30$). The beam is assumed to be uniform and undamped, with the mass per unit length, the stiffness, and the distance between the nodes of the FEM all set to unity. Six evenly spaced global nodes with displacement and rotational degrees of freedom are used, and so $n_g = 12$ and $n_e = 5$. To be consistent with the parallelism of the element/global hierarchy

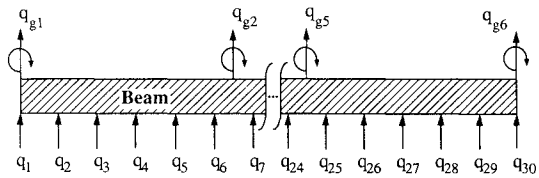

Fig. 5 30-node condensed beam model with collocated displacement, velocity sensors, and force actuators. There are six global nodes and five finite control elements.

of the structural model, the columns of the interpolation matrix T_g are developed from the same cubic polynomials used to form the original beam FEM.

The aim is to design a controller that minimizes a cost based on physical objectives that are motiviated by the typical performance goals of smart skins and mirror surfaces. Consequently, the state penalty is a summation of three terms, the LOS endpoint displacement pointing error, the squared displacement at each node, and the energy of the beam. Each actuator is penalized equally. With $\boldsymbol{x} = [\boldsymbol{q}^T \dot{\boldsymbol{q}}^T]^T$, the cost can be written as

$$J = \frac{1}{2}\int_0^\infty \left[\boldsymbol{x}^T R_{xx}\boldsymbol{x} + \boldsymbol{u}^T R_{uu}\boldsymbol{u}\right] \mathrm{d}t \tag{25}$$

with the condensed model weighting matrices

$$\boldsymbol{x}^T R_{xx}\boldsymbol{x} = \alpha_1(q_1 - q_n)^2 + \alpha_2 \sum_{i=1}^{n} q_i^2 + \alpha_3(\boldsymbol{q}^T K\boldsymbol{q} + \dot{\boldsymbol{q}}^T M\dot{\boldsymbol{q}}) \tag{26}$$

$$R_{uu} = \rho I_n \tag{27}$$

where $\alpha_1 = 1$, $\alpha_2 = 4/3$, $\alpha_3 = 0.025$, and $\rho = 1$ to place a relatively high weighting on the LOS and displacement penalties. As discussed in the preceding section, the performance objectives for the lower-level controller include only the displacement and energy weightings. The global controller can be obtained from an aggregated linear quadratic regulator (LQR) problem with consistently reduced state and control weighting matrices.[16]

As described in the synthesis algorithm in Ref. 16, the global control design ignores the stiffness coupling terms, namely, K_{gr} and K_{rg}, in Eq. (10). To study the effects of these terms on the overall design, a second controller for a global design model with only eight ($n_l = 8$) modes retained is also presented. As an indication of the decoupling that can be achieved, the closed-loop pole locations for the two central designs using a collocated local controller are plotted in Figs. 6 and 7. The open-loop poles refer to those of the condensed beam model with no control applied. The closed-loop poles are the poles of the condensed model with both the global and local controllers applied. The global design model poles represent the closed-loop poles of the uncoupled global design models. For clarity, the closed-loop poles of the residual design model are not shown, as they overlap the higher-frequency closed-loop poles. The improved agreement in Fig. 7 between the closed-loop poles and those predicted by the design models, when compared to those in Fig. 6, demonstrates the anticipated better decoupling between the models. However, it is also clear from Fig. 7 that retaining fewer global modes could result in a performance degradation if the lowest-frequency poles of the new residual model (essentially that part of the FEM not in the global model) are significantly removed from the optimal locations (shown by the global design model poles in Fig. 6). The use of more sophisticated local controllers will compensate for this performance loss.

The full hierarchic control architecture can be studied further by analyzing the tradeoffs between the achievable perfor-

Table 1 Comparison of the leading terms in the operations count for various local control designs

Controller type	Computations per finite control element (M or A)
Collocated	$2h_g$
Block diagonal	
Full	$2h_g^2$
Two bay	h_g^2
Block tridiagonal	
Full	$6h_g^2$
Banded width $= 2m + 1$	$(2m + 1)2h_g$

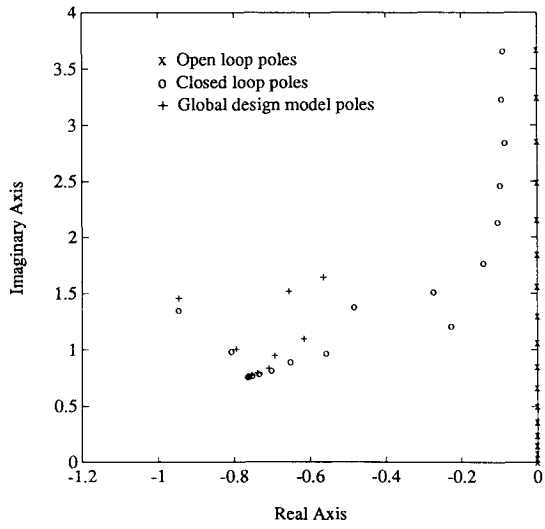

Fig. 6 Closed-loop poles when the hierarchic controller is applied to the beam design model ($n_g = 12$).

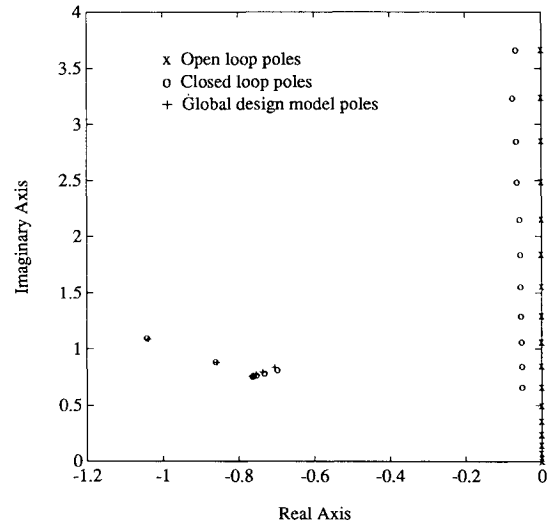

Fig. 7 Closed-loop poles when the hierarchic controller is applied to the beam design model using the alternative approach to improve decoupling ($n_g = 12$, $n_l = 8$)

mance and the required control effort (Fig. 8). The curves for the graph were obtained by simulating the closed-loop response of the beam model to an initial force disturbance at an arbitrary location. The simulated time traces provided the performance and control values used to determine the points on the curve. By definition, the optimal LQR controller represents the lowest achievable line on the graph. The performance curve for the uniform damping approach, which is the simplest of the decentralized control designs, is also drawn. The figure clearly illustrates the difference in performance between these two control approaches for this realistic cost function. The results obtained for the hierarchic controller designed using a global controller as discussed earlier and a local control based on uniform damping are also given in Fig. 8. The point marked ○ on the optimal curve corresponds to the design point ($\rho = 1$) for the global controller. This figure graphically shows the performance improvements that can be obtained by filtering the decentralized control and including the second level of control in the hierarchic architecture (Fig. 2).

To compare the other control methodologies, the same global design is combined with various local controllers, shown by the dotted lines in Fig. 8. There are now two important control parameters. Fixing the global control parameter ρ results in a locus of state/control points for various values of the local control parameter. For each value of the global parameter, there is an optimal point on the curve that minimizes the separation from the LQR boundary. Connecting these points then yields an appropriate cost curve for this combination of global and local approaches. For simplicity, the curves for only one global control design have been drawn. Although not apparent from the figure, the two block tridiagonal and full block diagonal designs provide comparable performance and are slightly superior to the two-bay block diagonal approach. However, it is apparent that for each design approach, the performance improvements are relatively small.

Figure 9 illustrates the results for the same local control designs combined with a central controller with only eight of the global modes retained. As discussed, the global and residual controllers exhibit much better decoupling, and so the closed-loop design model poles provide a better indication of the actual closed-loop poles. However, compared to the results in Fig. 8, the dotted curves on this graph are more widely separated, indicating larger differences in performance between the feedback methods. The larger spread between the curves for the various local designs confirms that, in this case,

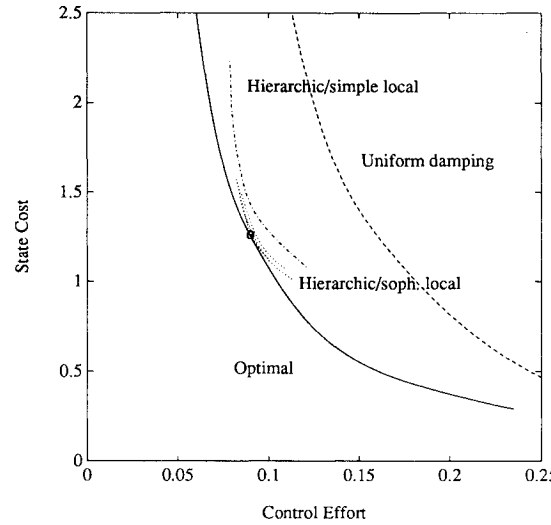

Fig. 8 Performance comparison of the various control designs ($n_g = 12$). The results for the more sophisticated local control designs are given by the dotted lines.

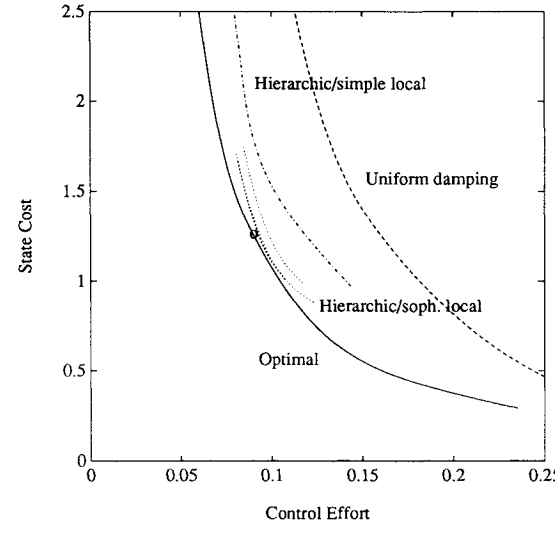

Fig. 9 Performance comparison of the various control designs with the improved decoupling ($n_g = 12$, $n_l = 8$). The results for the more sophisticated local control designs are given by the dotted lines.

Table 2 Operations count comparison

Controller type	30 nodes, $n_{gn}=6$	120 nodes, $n_{gn}=11$
Full state feedback $\sim\frac{8}{3}n^2$	2400	38,400
Global controller $\sim\frac{80}{3}n_{gn}^2$	960	3230
Architectural requirements per local controller	192	384
Collocated	16	32
Block diagonal		
Full	96	384
Two bay	48	192
Block tridiagonal		
Full	288	1152
Banded width = 5	80	160

Note: The second column corresponds to the example discussed, the third column corresponds to a larger example, local control values are per processor.

a more sophisticated local control design is necessary to obtain levels of performance comparable to the LQR approach.

The results in Figs. 8 and 9 are presented for only one set of α values in Eq. (26). The parameter α_1 has a significant influence on the central control design, and a larger value would widen the gap between the optimal and hierarchic designs in Fig. 9. The parameter α_2 influences both the global and local designs. A larger value would accentuate the suboptimality of the local control designs, resulting in a wider separation of the performances denoted by the dotted lines in Fig. 9. A larger α_2 value would also increase the difference between the performance of the hierarchic and LQR designs in Figs. 8 and 9. The parameter α_3 dominates the high response of the local controllers.

Another important aspect of the analysis is a comparison of the computaional requirements for the different local control approaches. The results presented here deal only with the number of computations required for the distributed control architecture. Other important issues, such as the communication between processors, are discussed in more detail in Refs. 14 and 43. The computational requirements for each of the local control designs are given in Table 1. The full set of results for two beam examples are given in Table 2.

For the local controllers, it is clear that using the full block tridiagonal feedback approach at the lower level is extremely expensive. The collocated approach requires the fewest number of computations in each case. The computational expense of the banded approach compared to the collocated design is directly related to the gain width required, but there are several comunication and implementation issues to be addressed with this tridiagonal design as well. As expected, Table 1 indicates that the full block diagonal approach is twice as expensive as the two-bay design, but Table 2 illustrates that, in both examples, the smaller block diagonal approach is on a par with the banded block tridiagonal design.

Several key conclusions can be drawn from the results in Table 2. First, there is overhead associated with the implementation of the architecture, and so the size of the system must be large to benefit from a hierarchic control design. Second, the processing requirements are highly distributed and parallel, which make them easier to achieve, but more complex to design and maintain. Finally, a large percentage of the calculations at the lower level are associated with the architecture and need only be performed at the much slower, global update rate.[19]

Conclusions

The results presented in this paper indicate that the hierarchic control architecture can give near optimal performance with a realistic objective in a computationally efficient manner. The performance objective in this case was physically motivated by goals typical of a control design for smart skins and mirror surfaces. Three local control design methodologies for symmetric structures were compared in terms of both performance vs control effort curves and the implementation requirements. The results with all modes retained in the global model were inconclusive, since introducing more sophisticated designs at the local level yielded marginal performance improvements over the results obtained with a very simple local design. However, as global modes were removed to improve subsystem decoupling, a reduction in performance was seen to occur for the less sophisticated local control approaches. If the size of the global model is selected (or reduced for improved decoupling) to be small enough that residual modes contribute significantly to the cost function, then to achieve the performance requirements, more sophisticated local controllers than collocated feedback should be utilized at the lower level.

Figures 8 and 9 demonstrate that, with either central design, the block diagonal and tridiagonal designs provide near optimal LQR performance. Consequently, a further conclusion is that, through an optimization procedure, it was possible to design isolated lower controllers that, when coupled to the global controller, yield a closed-loop performance comparable to those obtained with designs that require communication between the processors. This result has significant implications for simplifying the implementation procedure. The results demonstrated here also illustrate the utility of employing reduction techniques for designing decentralized controllers for symmetric structures such as mirrors.

The combined results also show that the two-bay block diagonal and the banded block tridiagonal designs are comparable in terms of computational requirements, but differ substantially in performance. In contrast, the full block diagonal and the banded block tridiagonal designs are comparable in terms of performance, but differ substantially in the computational requirements. Compared to the collocated design, all three approaches can offer much superior performance, but are significantly more expensive. It would appear that the optimized block diagonal methodologies are the most efficient in terms of performance and implementation requirements. However, the final decision as to which approach to use depends on the local processing power (i.e., the local rate at which calculations for the more sophisticated designs can be performed), the number of global modes retained in the central design model, the ease of locally communicating between processors, and the stringency of the performance objectives at the lower level.

Topics for further development include the analysis of the stability of the local control designs to asymmetric errors such as those that will occur during manufacturing and a combination of these results with the communications analysis in Ref. 43 to determine feasible processor architectures that will yield good closed-loop performance.

Acknowledgments

The research was supported by Air Force Office of Scientific Research Contract F49620-88-C-0015; by Edward F. Crawley's Presidential Young Investigators Award NSF Grant 84 51627-MSM; and by a 1967 Scholarship from the Natural Sciences and Engineering Research Council of Canada awarded to Jonathan How. The authors would like to thank Edward F. Crawley of the Massachusetts Institute of Technology for his help in this research.

References

[1]Junkins, J. L. (ed.), *Mechanics and Control of Large Flexible Structures,* Vol. 129, Progress in Aeronautics and Astronautics, AIAA, Washington, DC, 1990.

[2]Bahcall, J. (chairman), "A Decade of Discovery in Astronomy and Astrophysics," Rept. to the National Academy of Sciences, March 1991.

[3]Blackwod, G., Miller, D., and Jacques, R., "The MIT Multi-point Alignment Testbed: Technology Development for Optical Interferometry," *Proceedings of SPIE Conference on Active and Adaptive Optical Components,* San Diego, CA; International Society for Optical Engineering, Paper 1542-34, July 1991.

[4]How, J. P., Anderson, E. H., Miller, D. W., and Hall, S. R., "High Bandwidth Control for Low Area Density Deformable Mirrors," *Proceedings of SPIE Conference on Structures, Sensing and Control,* Orlando, FL; International Society for Optical Engineering, Paper 1489-19, April 1991.

[5]Aubrun J., Lorell, K., Mast, S., and Nelson, J., "Dynamic Analysis of the Actively Controlled Segmented Mirror of the W. M. Keck Ten-Meter Telescope," *IEEE Control Systems Magazine,* Vol. 5, No. 6, 1987, pp. 3-10.

[6]Chiarappa, D. J., and Claysmith, C. R., "Deformable Mirror Surface Control Techniques," *Journal of Guidance, Control, and Dynamics,* Vol. 4, No. 1, 1981, pp. 27-34.

[7]Hardy, J. W., "Active Optics: A New Technology for the Control of Light," *Proceedings of the IEEE,* Vol. 66, No. 6, 1978, pp. 651-697.

[8]Robertson, H. J., "Development of an Active Optics Concept Using a Thin Deformable Mirror," NASA CR-1593, March 1970.

[9]Wilson, R. N., Franza, F., and Noethe, L., "Active Optics I. A System for Optimizing the Optical Quality and Reducing the Costs of Large Telescopes," *Journal of Modern Optics,* Vol. 34, No. 4, 1987, pp. 485-509.

[10]Anderson, E. H., and How, J. P., "Implementation Issues in the Control of a Flexible Mirror Testbed," *Proceedings of SPIE Conference on Active and Adaptive Optical Components,* San Diego, CA; International Society for Optical Engineering, Paper 1542-35, July 1991.

[11]Bailey, T., and Hubbard, J. E., Jr., "Distributed Piezoelectric-Polymer Active Vibration Control of a Cantilever Beam," *Journal of Guidance, Control, and Dynamics,* Vol. 8, No. 5, 1985, pp. 605-611.

[12]Crawley, E. F., and Anderson, E., "Detailed Models of Piezoelectric Actuation of Beams," *Proceedings of the AIAA/ASME 30th Structures, Structural Dynamics, and Materials Conference,* AIAA, Washington, DC, April 1989.

[13]Hanagud, S., Obal, M., and Calise, A., "Piezoceramic Devices and PVDF Films as Sensors and Actuators for Intelligent Materials," *Proceedings of the U.S. Army Research Office Workshop on Smart Materials, Structures, and Mathematical Issues,* Virginia Polytechnic Inst. and State Univ., Blacksburg, VA, Sept. 1988, pp. 69-75.

[14]Crawley, E. F., How, J. P., and Warkentin, D., "Analytical and Experimental Issues in the Design of Intelligent Structures," *Proceedings of the Fourth NASA/DoD Control/Structures Interaction Technology Conference,* Orlando, FL, Nov. 1990, pp. 365-389, WL-TR-91-3013.

[15]Cantoni, V., and Levialdi, S. (eds.), "Pyramidal Systems for Computer Vision," *Proceedings of the NATO Advanced Research Workshop on Pyramidal Systems for Image Processing and Computer Vision,* Maratea, Italy, Springer Verlag, New York, May 1986.

[16]Hall, S. R., Crawley, E. F., How, J. P., and Ward, B., "A Hierarchic Control Architecture for Inteligent Structures," *Journal of Guidance, Control, and Dynamics,* Vol. 14, No. 3, 1991, pp. 503-512.

[17]Jamshidi, M., *Large-Scale Systems Modelling and Control,* Vol. 9, Series in System Science and Engineering, North-Holland, New York, 1983.

[18]Chow, J. H. (ed.), *Time-Scale Modeling of Dynamic Networks with Applications to Power Systems,* Lecture Notes In Control and Information Sciences, Vol. 46, Springer-Verlag, New York, 1982.

[19]How, J. P., "Local Control Design Methodologies for a Hierarchic Control Architecture," S.M. Thesis, Dept. of Aeronautics and Astronautics, Massachusetts Inst. of Technology, Cambridge, MA, Feb. 1990; also Space Engineering Research Center, Rept. 5-90.

[20]Ward, B., "A Hierarchical Control Architecture for Large Flexible Structures," S.M. Thesis, Dept. of Aeronautics and Astronautics, Massachusetts Inst. of Technology, Cambridge, MA May 1985; also Space Systems Lab., Rept. 18-85.

[21]Guyan, R., "Reduction of the Stiffness and Mass Matrices," *AIAA Journal,* Vol. 3, No. 2, 1965, p. 380.

[22]Skelton, R., Hughes, P., and Hablani, H., "Order Reduction for Models of Space Structures Using Modal Cost Analysis," *Journal of Guidance and Control,* Vol. 5, No. 4, 1982, pp. 351-357.

[23]Aubrun, J., "Theory of the Control of Structures by Low-Authority Controllers," *Journal of Guidance and Control,* Vol. 3, No. 5., 1980, pp. 444-451.

[24]Arbel, A., and Gupta, N., "Robust Collocated Control for Large Flexible Space Structures," *Journal of Guidance, Control, and Dynamics,* Vol. 4, No. 5, 1981, pp. 480-486.

[25]Joshi, S., "Robustness Properties of Collocated Controllers for Flexible Spacecraft," *Journal of Guidance, Control, and Dynamics,* Vol. 9, No. 1, 1986, pp. 85-91.

[26]Silverberg, L., "Uniform Damping Control of Spacecraft," *Journal of Guidance, Control, and Dynamics,* Vol. 9, No. 2, 1986, pp. 221-227.

[27]Sandell, N., Varaiya, P., Athans, M., and Safonov, M., "Survey of Decentralized Control Methods for Large Scale Systems," *IEEE Transactions on Automatic Control,* Vol. AC-23, No. 2, April 1978, pp. 108-128.

[28]Šiljak, D., *Large-Scale Dynamic Systems,* Series in System Science and Engineering, North-Holland, New York, Vol. 3, 1978.

[29]Levine, W., and Athans, M., "On the Determination of the Optimal Constant Output Feedback Gains for Linear Multivariable Systems," *IEEE Transactions on Automatic Control,* Vol. AC-15, No. 1, Feb. 1970, pp. 44-48.

[30]Petkovski, D. J., and Rakic, M., "On the Calculation of Optimum Feedback Gains for Output Constrained Regulators," *IEEE Transactions on Automatic Control,* Vol. AC-23, No. 4, Aug. 1978, p. 760.

[31]Guardabassi, G., Locateli, A., Maffezzoni, C., and Schiavoni, N., "A Parameter Optimization Approach to Computer-Aided Design of Structurally Constrained Multivariable Regulators," *Control and Computers,* Vol. 10, No. 1, 1983, pp. 39-49.

[32]Ly, U.-L., "A Design Algorithm for Robust Low-Order Controllers," Stanford Univ., Stanford, CA, SUDAAR 536, Nov. 1982.

[33]Chu, K.-C., "Optimal Decentralized Regulator for a String of Coupled Systems," *IEEE Transactions on Automatic Control,* Vol. AC-19, No. 3, June 1974, pp. 243-246.

[34]Brockett, R. W., and Willems, J. L., "Discretized Partial Differential Equations: Examples of Control Systems Defined on Modules," *Automatica,* Vol. 10, No. 5, 1974, pp. 507-515.

[35]Wall, J., "Control and Estimation for Large-Scale Systems Having Spatial Symmetry," Ph.D. Thesis, Dept. of Electrical Engineering and Computer Science, Massachusetts Inst. of Technology, Cambridge, MA, Aug. 1978.

[36]de Luis, J., "Design and Implementation of Optimal Controllers for Intelligent Structures Using Infinite Order Structural Models," Ph.D. Dissertation, Dept. of Aeronautics and Astronautics, Massachusetts Inst. of Technology, Cambridge, MA, Jan. 1989; also Space Systems Lab., Rept. 3-89.

[37]Lunze, J., "Stability Analysis of Large-Scale Systems Composed of Strongly Coupled Similar Subsystems," *Automatica,* Vol. 25, 1989, pp. 561-570.

[38]Graham, A., *Kronecker Products and Matrix Calculus: with Applications,* Ellis Horwod, New York, 1981.

[39]Mercadal, M., "H_2 Fixed Architecture, Control Design Methodology for Large Scale Systems," Ph.D. Dissertation, Dept. of Aeronautics and Astronautics, Massachusetts Inst. of Technology, Cambridge, MA, June 1990.

[40]Kronsjö, L., *Algorithms: Their Complexity and Efficiency,* Wiley-Interscience, New York, 1987.

[41]Haddad, W. M., Bernstein, D. S., and Nett, C. N., "Decentralized H_2/H_∞ Controller Design: The Discrete-Time Case," *Proceedings of the IEEE Conference on Decision and Control,* Tampa, FL, Dec. 1989, pp. 932-933.

[42]MacMartin, D. G., Hall, S. R., and Bernstein, D. S., "Fixed Order Multi-Model Estimation and Control," *Proceedings of the 1991 American Control Conference,* Inst. of Electrical and Electronics Engineers, Piscataway, NJ, June 1991, pp. 2113-2118.

[43]Warkentin, D., "Embedded Electronics for Intelligent Structures," S.M. Thesis, Dept. of Aeronautics and Astronautics, Massachusetts Inst. of Technology, Cambridge, MA, April 1991; also Space Engineering Research Center, Rept. 2-91.